

Stage-Structured Infection Transmission and a Spatial Epidemic: A Model for Lyme Disease

Thomas Caraco,^{1,*} Stephan Glavanakov,¹ Gang Chen,² Joseph E. Flaherty,² Toshiro K. Ohsumi,² and Boleslaw K. Szymanski²

1. Department of Biological Sciences, University at Albany, Albany, New York 12222;

2. Department of Computer Science, Rensselaer Polytechnic Institute, Troy, New York 12180

Submitted June 5, 2000; Accepted February 15, 2002

ABSTRACT: A greater understanding of the rate at which emerging disease advances spatially has both ecological and applied significance. Analyzing the spread of vector-borne disease can be relatively complex when the vector's acquisition of a pathogen and subsequent transmission to a host occur in different life stages. A contemporary example is Lyme disease. A long-lived tick vector acquires infection during the larval blood meal and transmits it as a nymph. We present a reaction-diffusion model for the ecological dynamics governing the velocity of the current epidemic's spread. We find that the equilibrium density of infectious tick nymphs (hence the risk of human disease) can depend on density-independent survival interacting with biotic effects on the tick's stage structure. The local risk of infection reaches a maximum at an intermediate level of adult tick mortality and at an intermediate rate of juvenile tick attacks on mammalian hosts. If the juvenile tick attack rate is low, an increase generates both a greater density of infectious nymphs and an increased spatial velocity. However, if the juvenile attack rate is relatively high, nymph density may decline while the epidemic's velocity still increases. Velocities of simulated two-dimensional epidemics correlate with the model pathogen's basic reproductive number (R_0), but calculating R_0 involves parameters of both host infection dynamics and the vector's stage-structured dynamics.

Keywords: Lyme disease, population structure, reaction-diffusion model, spatial dynamics, spatial velocity.

A basic ecological property of an emerging disease, or of any invasive species, is the speed at which its range expands (Murray et al. 1986; Andow et al. 1990; Holmes et al. 1994). An epidemic's spatial velocity depends on mech-

anisms of pathogen dispersal and on the population dynamics of infection transmission (van den Bosch et al. 1990; Mollison 1991; Clark et al. 2001). We model a vector-borne disease where the vector's stage structure affects the transmission dynamics and so affects epidemic velocity.

Most models for vector-borne disease ignore vector population dynamics. If the vector's lifespan is much shorter than its host's, the frequency of pathogen-infected vectors may equilibrate quickly (Aron and May 1982), and disease among hosts can be predicted without modeling the vector explicitly (Dye and Williams 1995). But if host and vector have a similar lifespan, infection-transmission rates and the velocity at which disease spreads depend on the coupled dynamics of host and vector densities (Feng and Velasco-Hernández 1997). Furthermore, for certain vector-borne diseases, infection transmission requires that the vector progress through a developmental transition. For these cases, the vector's stage-structured dynamics should govern the spatial expansion of infection (Neubert and Caswell 2000).

An example is the cycle of infection associated with Lyme disease (Barbour and Fish 1993; White 1998). The 2-yr life cycle of the vector, a tick, scales similarly with the lifespan of its mammalian hosts. Larval ticks acquire the infection at the first blood meal, progress to the nymph stage, and then may infect a host at the second meal. So, analyzing the spread of infection suggests consideration of the vector's stage-structured population dynamics (Awerbuch and Sandberg 1995; Van Buskirk and Ostfeld 1995; Caraco et al. 1998).

In the northeast United States, the geographic range of human Lyme disease has increased steadily (White et al. 1991) as high rates of infection expand from disease foci (Glavanakov et al. 2001). We model the advance of the natural infection cycle as a reaction-diffusion process. The model may help identify factors influencing the rate at which the disease spreads, and more generally, it emphasizes that population structure may affect the spatial dynamics of ecological interactions (Diekmann et al. 1998; Neubert and Caswell 2000).

* E-mail: caraco@csc.albany.edu.

Lyme Disease: Ecological Background

Lyme disease in the northeast United States involves interactions among no fewer than four species (Ostfeld et al. 1995; Jones et al. 1998). The pathogen is a spirochetal bacterium *Borrelia burgdorferi*. The hematophagous vector is the black-legged tick *Ixodes scapularis*. Most newly hatched larvae attack white-footed mice *Peromyscus leucopus*; a few larvae attack other hosts (Spielman et al. 1985). Replete larvae molt and winter as nymphs. At the start of the second year, surviving nymphs “quest” for a second blood meal. Most successful nymphs again attack mice, but some infectious nymphs bite humans. After feeding on mice, nymphs quickly mature as adults. Adult ticks feed preferentially on white-tailed deer *Odocoileus virginianus*, and mating occurs on deer. Mated females eventually drop off the deer, winter in leaf litter, oviposit, and then die. In different geographic regions, the hosts, vectors, and strains of *Borrelia* may differ, but the cycle of infection usually has the same qualitative properties (Bennett 1995).

Mice do not transmit *Borrelia* vertically. They are infected only by tick bites and apparently do not recover from infection (Burgess et al. 1993). Piesman (1988) indicates that only 0.1% of ticks is infected transovarially, although the figure differs among tick-*Borrelia* associations (Bennett 1995). Maintenance of the spirochete is due primarily to the tick-mouse cycle of infection. Seasonal abundance of the tick developmental stages helps drive the cycle. In general, nymphs infected last year appear first; these ticks transmit *Borrelia* to susceptible mice. Later in the same year, larvae hatch (i.e., the next tick generation appears) and may acquire the pathogen when they feed on recently infected mice.

Deer dispersal influences the spatial pattern of tick larvae, since deer move fecund adult ticks (Wilson et al. 1990). But deer do not disperse the pathogen. Deer cannot be infected, and transovarial transmission in ticks is rare. Furthermore, *Borrelia* cannot survive outside of its hosts (Barbour and Fish 1993). Mice ordinarily disperse juvenile ticks, and dispersal of infectious mice can introduce the spirochete into tick populations. So the spatial advance of infection must be driven by dispersal of mice and other hosts to juvenile ticks (Van Buskirk and Ostfeld 1998). Our model formalizes this observation in a manner predicting the velocity at which spirochete infection advances spatially.

A Reaction-Diffusion Model for Lyme Disease

Our model treats population densities at locations (x, y) in a continuous two-dimensional space Ω . Parameters for birth, death, infection, and developmental advance do not

depend on spatial location. Diffusion approximates dispersal via random motion (Holmes et al. 1994).

No current evidence suggests that tick infestation or *Borrelia* infection affects mortality or fecundity in mice (Gage et al. 1995). So, we assume the dynamics and dispersal of mice are independent of infestation/infection status. To limit the number of variables, we ignore dispersal of nymphs. At equilibrium population densities, nymph dispersal does not affect the spread of Lyme disease. Dispersal of larvae is, however, important; spatial dispersion of replete larvae governs the pattern in the risk of Lyme disease when these animals quest as nymphs (Mather 1993). Therefore, we model dispersal of larvae while they feed on mice.

Adult ticks reproduce and disperse diffusively; dispersal of adults mimics movements of deer while ticks mate (deer are not modeled explicitly). Natality and mortality among black-legged ticks are apparently independent of *Borrelia* infection (Van Buskirk and Ostfeld 1998).

We assume continuous time, approximating the natural system from spring through late summer. Our assumptions ignore seasonal pattern in tick abundance; see Caraco et al. (1998). The model requires six state variables for the reaction-diffusion dynamics. Three subsidiary variables are required to model the tick’s population structure. Table 1 lists all parameters.

Mice reproduce in a density-dependent manner and incur density-independent mortality. Since mice are born uninfected, the equation for susceptible-mouse density $M(x, y, t)$ includes birth, death, acquisition of the spirochete from infectious-nymph bites, and dispersal:

Table 1: Parameters of the reaction-diffusion model

Parameter	Definition
r_M	Maximal individual birthrate in mice
K_M	Carrying capacity for mice
μ_M	Mortality rate per mouse
D_M	Diffusion coefficient for mice
D_H	Diffusion coefficient for deer
r	Maximal individual birthrate in ticks
c	Crowding coefficient in ticks
μ_L	Mortality rate per questing tick larva
μ_V	Mortality rate per feeding tick larva
μ_N	Mortality rate per tick nymph
μ_A	Mortality rate per adult tick
α	Attack rate, juvenile ticks on mice
γ	Attack rate, tick nymphs on humans
β	Susceptibility to infection in mice
β_T	Susceptibility to infection in ticks
σ	Rate at which larvae complete first blood meal
ξ_0	Standardized velocity of wave front

$$\frac{\partial M(x, y, t)}{\partial t} = r_M(M + m) \left(1 - \frac{M + m}{K_M} \right) - \mu_M M - \alpha \beta M n + D_M \left(\frac{\partial^2 M}{\partial x^2} + \frac{\partial^2 M}{\partial y^2} \right), \quad (1)$$

where r_M is the intrinsic birthrate; K_M is the spatially homogeneous carrying capacity; μ_M is the individual mortality rate among mice; α is the “attack rate” of juvenile ticks questing for mice; β ($0 < \beta < 1$) is a mouse’s susceptibility to pathogen infection when bitten by an infectious nymph; and D_M is the diffusion coefficient for mice, with units (distance)²/time.

The density of pathogen-infected mice $m(x, y, t)$ increases as susceptible mice are bitten by infectious nymphs and decreases through mortality. The equation for infected mice includes infection, death, and dispersal:

$$\frac{\partial m(x, y, t)}{\partial t} = \alpha \beta M n - \mu_M m + D_M \left(\frac{\partial^2 m}{\partial x^2} + \frac{\partial^2 m}{\partial y^2} \right). \quad (2)$$

The subsidiary variable $L(A, a)$ is the density of questing larvae. We assume that larval hatching rate depends nonlinearly on adult tick density; for discussion of the assumed self-regulation in ticks, see Sutherst et al. (1973), Randolph (1994), or Hughes and Randolph (2001). The density of questing larvae declines through mortality and attacks on mice. Then, at each (x, y) :

$$\frac{dL}{dt} = r(A + a)[1 - c(A + a)] - \mu_L L - \alpha L(M + m), \quad (3)$$

where r is the tick’s per capita reproduction at low density; μ_L is the mortality rate among questing larvae; and c represents crowding among reproducing ticks. Larvae must hatch at a positive rate when $(A + a) > 0$, so we assume c is small. Essentially, c is inversely proportional to deer density, which is assumed a constant and treated implicitly.

Given densities of questing larvae, the density of larvae infesting susceptible mice, $V(x, y, t)$, changes through successful attack, completion of the first blood meal, death, and dispersal while they infest mice:

$$\frac{\partial V(x, y, t)}{\partial t} = \alpha M L - V(\sigma + \mu_V) + D_M \left(\frac{\partial^2 V}{\partial x^2} + \frac{\partial^2 V}{\partial y^2} \right), \quad (4)$$

where σ is the rate at which larvae infesting mice complete their meal, and μ_V is the mortality rate among larvae infesting mice. Since the duration of a larval meal seldom exceeds a few days (Barbour and Fish 1993), $\sigma > \mu_V$. The assumptions concerning the density of larvae infesting

pathogen-infected mice, $v(x, y, t)$, are similar. We substitute the density of infectious mice (m) for susceptible-mouse density (M) and obtain $\partial v(x, y, t)/\partial t$.

The subsidiary variable $N(V, v)$ is the density of susceptible questing nymphs at (x, y, t) . The variable $N(V, v)$ increases as larvae complete their first meal without acquiring the spirochete. The larvae may have infested a susceptible mouse or attacked an infectious mouse and avoided infection. As they die, bite humans, and attack mice, $N(V, v)$ decreases. Combining processes yields

$$\frac{dN}{dt} = \sigma[V + (1 - \beta_T)v] - N[\gamma + \alpha(M + m) + \mu_N], \quad (5)$$

where β_T is a tick’s susceptibility to infection when feeding on an infected mouse; $0 < \beta_T < 1$. The mortality rate among questing nymphs is μ_N , and γ is the rate at which nymphs bite humans.

The subsidiary variable $n(v)$ is the density of questing, infectious nymphs at (x, y, t) . Infectious nymphs must have attacked a mouse infected with *Borrelia* as larvae and then acquired the pathogen. Their density at any location (x, y) varies as

$$\frac{dn}{dt} = \beta_T \sigma v - n[\gamma + \alpha(M + m) + \mu_N]. \quad (6)$$

The term $\gamma n(x, y, t)$ represents the local risk of Lyme disease to humans. We assume that nymphs biting humans do not feed long enough to mature as adults.

Given densities of susceptible nymphs $N(x, y, t)$, the density of uninfected adult ticks $A(x, y, t)$ changes through attacks of those nymphs on mice, death of adults, and dispersal:

$$\frac{\partial A(x, y, t)}{\partial t} = \alpha N[M + (1 - \beta_T)m] - \mu_A A + D_H \left(\frac{\partial^2 A}{\partial x^2} + \frac{\partial^2 A}{\partial y^2} \right), \quad (7)$$

where μ_A is the density-independent mortality rate among adult ticks. The diffusion coefficient D_H models dispersal of adult ticks while they infest deer.

Given densities of infectious nymphs $n(x, y, t)$, the density of pathogen-infected adult ticks $a(x, y, t)$ increases as infected nymphs attack any mouse and as susceptible nymphs attack infected mice and acquire *Borrelia* during their second blood meal. Adding death and dispersal, we have

$$\frac{\partial a(x, y, t)}{\partial t} = \alpha[(M + m)n + \beta_T mN] - \mu_A a + D_H \left(\frac{\partial^2 a}{\partial x^2} + \frac{\partial^2 a}{\partial y^2} \right). \quad (8)$$

Traveling Wave Conjecture

Suppose that a local population exhibits positive per capita growth at low density, self-regulation, and that diffusion occurs along one dimension. The equilibria of local growth are 0 and K , the carrying capacity. If initial density is 0 everywhere and a small density is introduced at one location, that population will increase to K locally and expand as a traveling wave. As the wave advances spatially, it transforms the first equilibrium (0) into the positive equilibrium K . The wave has asymptotic speed $(4\rho D)^{1/2}$, where ρ is the intrinsic rate of increase and D is the diffusion coefficient (Murray et al. 1986; Holmes et al. 1994; Dwyer and Elkinton 1995). Qualitatively similar traveling waves can characterize stage-structured populations (Neubert and Caswell 2000) and multispecies reaction-diffusion systems (Dunbar 1983; Hutson 1986).

Reaction Equilibria

To analyze our model, we first identify the aspatial equilibria. After deleting diffusion terms, the equations yield three such equilibria: extinction of the system, positive abundance of ticks and mice in the absence of the spirochete, and proportional infection of both mice and ticks. The appendix gives conditions for feasibility of the equilibria and their local stability.

Several equilibrium values depend on the total (susceptible plus infected) density of mice or on the total density of adult ticks. At positive equilibrium, the total density of mice is

$$M^* + m^* = K_M \left(1 - \frac{\mu_M}{r_M} \right) = Q, \quad (9)$$

where Q is a convenience. If $r_M > \mu_M$, Q is stable. Total density of adult ticks at equilibrium is

$$A^* + a^* = \frac{1}{c} - \frac{(\alpha Q + \mu_L)(\sigma + \mu_V)(\gamma + \alpha Q + \mu_N)\mu_A}{rc\sigma(\alpha Q)^2}, \quad (10)$$

where $c < 1$. Increases in αQ , the rate at which each individual juvenile tick attacks mice, can increase adult tick density. A milder abiotic environment should reduce the juvenile mortality rates and so increase adult tick density.

Given total mouse and adult tick densities, we can obtain positive equilibrium levels for individual state variables. The equilibrium density of pathogen-infected mice, m^* , is

$$m^* = Q \frac{\beta_T \mu_A (A^* + a^*) - \mu_M Q}{\beta_T \mu_A (A^* + a^*)}. \quad (11)$$

Maintaining the cycle of infection requires $m^* > 0$. Intuitively, geometric mean susceptibility to infection, $(\beta_T)^{1/2}$, must be sufficiently high. The appendix shows that maintaining *Borrelia* infection requires a greater r than does maintaining a tick population at equilibrium in the absence of infection. For most juvenile-mortality combinations and given r/μ_A , an increased equilibrium density of mice makes infection-cycle maintenance more likely.

The variable most important in predicting the risk of human Lyme disease is the density of infectious nymphs n^* :

$$n^* = \frac{\beta_T \mu_A (A^* + a^*) - \mu_M Q}{\beta_T \alpha Q}. \quad (12)$$

The positive equilibrium densities for the remaining seven variables of the model are listed in table 2.

Table 2: Positive equilibrium densities

Susceptible mice	$M^* = Q - m^* = \mu_M Q^2 / [\beta_T \mu_A (A^* + a^*)]$
Questing larvae	$L^* = \{[(\sigma + \mu_V)(\gamma + \alpha Q + \mu_N)\mu_A] / \sigma(\alpha Q)^2\} (A^* + a^*)$
Larvae on infected mice	$v^* = [(\gamma + \alpha Q + \mu_N) / \sigma \alpha Q] \{[\beta_T \mu_A (A^* + a^*) - \mu_M Q] / \beta_T\}$
Larvae on susceptible mice	$V^* = [\mu_M (\gamma + \alpha Q + \mu_N)] / \beta_T \alpha \sigma$
Susceptible nymphs	$N^* = \{[\mu_A (1 - \beta_T) / \alpha Q] (A^* + a^*)\} + (\mu_M / \alpha \beta)$
Infected adult ticks	$a^* = (\alpha / \mu_A) [Q n^* + \beta_T m^* N^*]$
Uninfected adult ticks	$A^* = (\alpha / \mu_A) N^* (Q - \beta_T m^*)$

Note: The text gives total mice (Q), infected mice (m^*), total adult ticks ($A^* + a^*$), and infectious nymphs (n^*). Note that both a^* and A^* can be expressed directly in terms of model parameters by substituting for N^* and then using equation (10).

Before analyzing the diffusion model's velocity, we summarize properties of the aspatial equilibrium and its stability. Figure 1A shows how the equilibrium density of infectious nymphs n^* can depend on adult tick mortality rate μ_A . In each plot, n^* reaches a maximum at some intermediate μ_A . High adult tick mortality, which could result from either severe weather or application of an acaricide to deer (Pound et al. 2000), reduces each juvenile tick density as the number of reproductive ticks declines. Very low adult mortality can reduce juvenile tick density through the assumed density dependence in tick reproduction.

Comparing plots in figure 1A shows that decreasing juvenile tick mortality rates not only increases n^* but also increases the maximal adult mortality μ_A allowing a positive equilibrium density of infectious nymphs. So, the three plots collectively indicate that the risk of Lyme disease should depend on the way abiotic factors influencing tick mortality interact with crowding during reproduction.

For each plot in figure 1A, the total density of ticks (combining stage and infection status) varies little over low and intermediate levels of μ_A , and then declines rapidly with n^* at high μ_A . Stage structure, in contrast, varies smoothly; the relative abundance of the juvenile tick stages increases with any increase in μ_A , until there are too few adults to maintain positive equilibrium.

Figure 1B shows how n^* can depend on the juvenile tick attack rate α . In each plot, n^* reaches a maximum at an intermediate α . When the attack rate is very low, most larvae die before feeding. A much larger α sufficiently reduces the length of time a nymph quests for a blood meal to decrease the density of infectious nymphs. Total tick density initially increases with α and then remains relatively large across higher levels of the attack rate. Hence, both total density and the tick population's stage structure vary significantly as α increases.

The model's positive equilibrium densities suggest that n^* and the risk of Lyme disease to humans are greatest at intermediate adult tick mortality μ_A and intermediate attack rate α . However, the density of infected mice m^* (not shown in fig. 1) exhibits a different pattern; m^* responds to variation in adult mortality, as does n^* , but it does not follow that a high density of infectious nymphs is always required for a high frequency of infection among mice. As attack rate α increases, m^* increases monotonically despite the decrease in n^* at higher α . Below, we show that the velocity of the spatial epidemic qualitatively matches the pattern of infection frequency in mice, rather than the pattern in the density of infectious nymphs.

Stability of Vector Stage Structure

Assuming that total mouse density remains at equilibrium, we consider local stability of the tick's equilibrium stage

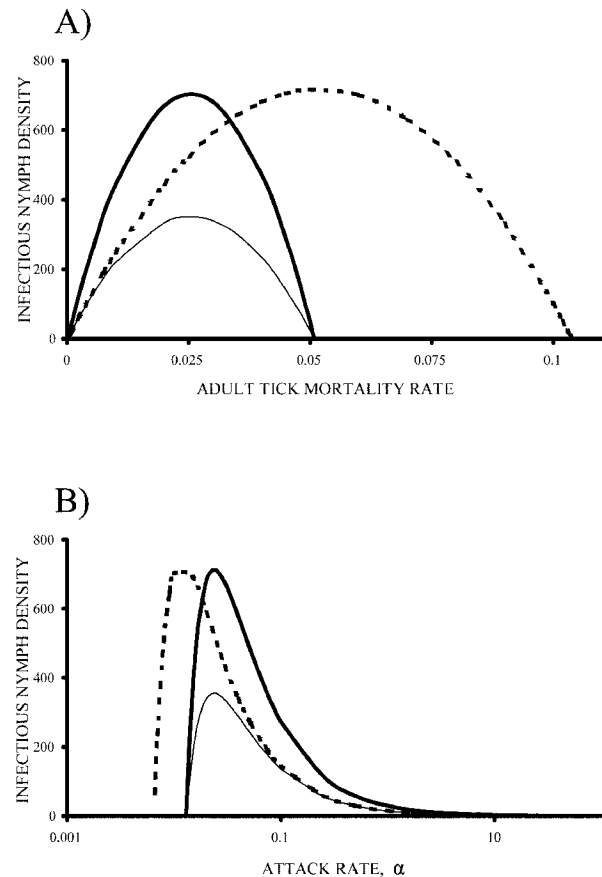


Figure 1: Infectious nymph density at equilibrium. *A*, n^* against adult tick mortality rate. *Thick line:* base-level parameters ($Q = 3$, $\mu_M = 0.02$, $r = 0.35$, $c = 0.0003$, $\gamma = 0.005$, $\sigma = 0.25$, $\alpha = 0.02$, $\mu_L = 0.09$, $\mu_V = 0.08$, $\mu_N = 0.06$). *Thin line:* juvenile tick mortalities halved; other parameters at base level. *Broken line:* c halved; other parameters at base level. *B*, n^* against attack rate, α . $\mu_A = 0.03$ in each plot; otherwise, parameters varied among three plots as in *A*.

structure without reference to infection, since *Borrelia* does not affect tick demography. The total densities ($A^* + a^*$), L^* , ($N^* + n^*$), and ($V^* + v^*$) specify the tick's stage structure. Equilibria are extinction of the tick population and the positive equilibrium densities.

The appendix indicates that for any given adult mortality rate μ_A or any given attack rate α , stability depends on the tick intrinsic birthrate r . If r is sufficiently small, extinction is locally stable, and the positive equilibrium is not feasible. As r increases, positive equilibrium densities become feasible and locally stable, and extinction is unstable. As r continues to increase, both extinction and the positive equilibrium are unstable, and the tick densities begin to cycle.

Stability of Infection Equilibria

Next, we examine the condition for *Borrelia*'s invasion of the tick-mouse interaction at demographic equilibrium. The infection equilibria are extinction of the spirochete, and the positive equilibrium $[m^*v^*n^*a^*]$. We assume mouse density remains at positive equilibrium and that total tick densities remain at the positive stage-structured equilibrium. The appendix shows that whenever $m^* > 0$ is feasible, the infection equilibrium is locally stable. Otherwise, extinction of the spirochete is stable. From the appendix, local stability of spirochete extinction requires

$$\mu_M Q > \beta \beta_T \mu_A (A^* + a^*). \tag{13}$$

That is, the spirochete cannot advance when rare, and the tick densities remain at demographic equilibrium, when the number of mice dying exceeds the number of adult ticks dying times the product of the mouse and tick susceptibilities. In areas where spirochete infection is enzootic, tick densities are far greater than mouse density (Ostfeld et al. 1998), and adult tick densities in our model increase with the density of mice, by equation (10).

We verify the stability criterion for the infection dynamics by evaluating R_0 , the number of infections per infection when the spirochete is rare. The disease advances initially if $R_0 > 1$. Since the infection process involves vector and host dynamics, we calculate R_0 in stages.

Suppose an initial infectious nymph enters the tick-mouse system at demographic equilibrium. The nymph attacks, at most, one mouse. Given that the nymph feeds before it dies, the probability of infecting the host is β . The expected number of mice infected by this nymph, R_n , is the unconditional probability that *Borrelia* is transmitted to a single mouse:

$$R_n = \frac{\beta \alpha Q}{(\gamma + \alpha Q + \mu_N)} < 1. \tag{14}$$

If a mouse acquires the spirochete from the first infected nymph, R_m is the expected number of nymphs infected, as feeding larvae, by that mouse. Larvae attack the mouse at rate αL^* during its remaining lifetime, a fraction β_T are infected, and a fraction $\sigma/(\sigma + \mu_V)$ survive to quest as nymphs. Then,

$$R_M = \frac{\beta_T \sigma \alpha L^*}{(\sigma + \mu_V) \mu_M}. \tag{15}$$

The number of infections/initial infection is $R_0 = R_n R_m$, which can be expressed as

$$R_0 = \frac{\beta \beta_T \mu_A A^*}{\mu_M Q}, \tag{16}$$

where $A^* = (A^* + a^*)$ when infection is rare. The criterion for advance of the infection, $R_0 > 1$, just reverses the condition for stability of the spirochete's extinction.

Spatial Velocity of Infection

Next we ask how adult tick mortality and juvenile attack rate influence the velocity at which infection spreads in the diffusion model (van den Bosch et al. 1990; Dwyer 1994). We assume demographic equilibrium and introduce infectious nymphs in a small area within the space Ω where neither mice nor other ticks are infected. If the pathogen advances, infection should spread as a circular wave front about the inoculum (Lewis and Kareiva 1993). As time grows large, the wave front should approach a constant velocity. As the wave passes any location, densities of infected ticks and infectious mice should increase until, we assume, they attain the positive equilibrium levels. The initial wave-front velocity may be lower in two dimensions than in one dimension (Holmes et al. 1994), but we can approximate the velocity using one-dimensional models (Murray et al. 1986; Dwyer 1994). We apply a method from Mollison (1991), which may be consulted for details. The method invokes a linear approximation of the dynamics, so that R_0 approximates the number of infected tick nymphs per infection cycle. Furthermore, our velocity analysis treats space as one-dimensional.

The velocity at which disease spreads depends first on R_0 , second, on spatial locations where ticks are infected as larvae, which itself depends on diffusion of infected mice, and, finally, on the average duration of the cycle of infection (Mollison and Levin 1995). Since R_0 is discussed above, we turn to the locations of infection.

The continuous random variable X represents the distance between the location where a mouse acquires infection and the location where it transmits infection to a larval tick. Under random diffusion, a cohort of mice infected at the same location produces a normal distribution of dispersing mice with an average displacement of 0. But the variance of the dispersal distance is proportional to $(D_M t)$, so the mean squared displacement increases with time.

Next, let the continuous random variable T represent the duration of a "typical" cycle of transmission from nymph to mouse to larva. In probabilistic terms, T is the sum of random waiting times. An infectious tick nymph quests for an interval with mean $\psi^{-1} = (\gamma + \alpha Q + \mu_N)^{-1}$. The probability that the waiting time ends with infection of a mouse is $\beta \alpha Q / \psi$. Given transmission of the

spirochete to the host, the time elapsing to a typical larval infection will have the same distribution as the mouse's remaining lifetime, since larvae attack randomly and independently; this is a key assumption (Mollison 1991). The mouse remains alive for an interval with mean μ_M^{-1} ; during this time, the mouse is attacked by larvae at constant probabilistic rate αL^* . A larva feeding on an infected mouse acquires *Borrelia* and survives to quest as an infectious nymph with combined probability $\beta_T \sigma / (\sigma + \mu_V)$. For simplicity, we ignore the larval meal, which lasts only a day or so. Then $E[T] = \psi^{-1} + \mu_M^{-1}$. Note that diffusion of *Borrelia* begins only after infection of the mouse (see Murray et al. 1986).

Let $K_0(X, T)$ be the joint probability density of distance X and cycle duration T . Then, the reproduction-dispersal kernel, or infection-dispersal kernel, is $K(X, T) = R_0 K_0(X, T)$, which combines the three elements listed above (van den Bosch et al. 1990). The appendix presents our analysis of wave-front velocity, which we express in a standardized form. That is, if ξ is a velocity, we write the standardized velocity as $\xi_0 = \xi E[T]^{1/2} / 2D_M^{1/2}$. Since D_M has units of (distance)²/time, ξ_0 is dimensionless (Mollison and Levin 1995).

Figure 2A shows how the standardized velocity of the advancing disease varies with adult tick mortality rate. In each plot, ξ_0 reaches a maximum as μ_A increases and then declines with further increases in μ_A . The value of R_0 for the disease responds similarly to variation in μ_A . Combining these effects with those associated with figure 1A, indicates that the important demographic quantities vary similarly (and nonmonotonically) with adult tick mortality: infectious nymphs, infected mice, the pathogen's R_0 , and the velocity at which disease advances spatially.

Figure 2B shows how standardized velocity depends on the juvenile tick attack rate α . In each plot, ξ_0 increases in a strictly monotonic, decelerating manner as α increases. R_0 for the pathogen varies similarly with α , as does the density of infected mice. Comparing these patterns with figure 1B indicates that at low α , the velocity at which disease spreads increases as the density of infectious nymphs increases. However, at higher levels of α , the epidemic's spatial velocity and the local risk of zoonotic infection, n^* , decouple. So, the velocity at which disease advances spatially always varies concordantly with the pathogen's R_0 and the density of infected hosts (the dispersers, m^*) but does not match variation in the density of infectious vectors (n^*).

We simulated the two-dimensional reaction-diffusion model using techniques that adaptively refine time and space steps to approximate the wave front (Adjerid et al. 1999; Ohsumi et al. 2000). We began with total densities of mice and tick stages at demographic equilibrium across a square region. We set densities of infected mice and

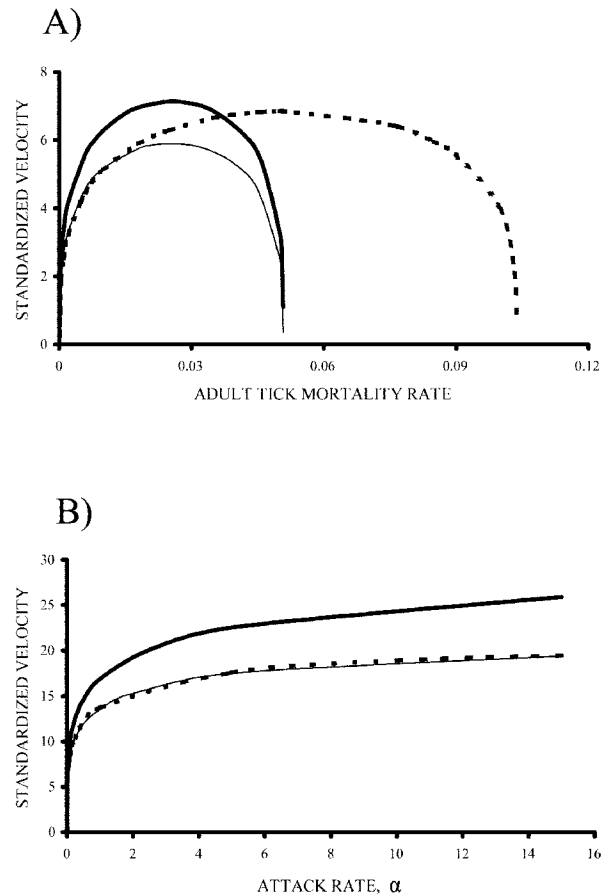


Figure 2: Approximated standardized velocities for diffusion of infection. $D_H = 0.1 = 10D_M$. A, ξ_0 against adult tick mortality rate μ_A ; base-level parameters as in figure 1A. B, ξ_0 against attack rate α ; base-level parameters as in figure 1B.

infected ticks at infection-equilibrium densities in a small square at the center of the region; elsewhere, no organisms were infected initially.

In six simulations, we chose parameter values where both the total tick densities and the predicted enzootic infection frequencies were locally stable. In each case, the densities of infected mice and infected ticks increased, via an advancing front, to equilibrium across the region. Observed equilibria are very close to the values given by the aspatial solution. Table 3 shows the predicted densities of infected mice and tick nymphs and the equilibria observed in simulation. It also shows predicted and observed velocities of the infection. Densities match well quantitatively. Velocities estimated from the simulations are lower, by 30% on average, than values predicted by the one-dimensional approximation, but the rank order of the estimated velocities and those solved from the model are the same.

Table 3: Comparison of model and simulation results

	μ_A			α		
	.002	.025	.045	.015	.02	.5
m^*	2.81	2.97	2.93	2.93	2.97	2.99
$m(s)$	2.81	2.97	2.93	2.93	2.97	2.99
n^*	50.04	350.09	141.76	184.76	338.93	29.03
$n(s)$	50.04	350.17	141.69	184.64	338.93	29.03
N^*	56.71	356.76	148.42	193.65	345.6	29.3
$N(s)$	56.71	356.84	148.36	193.52	345.59	29.3
ξ_0	2.31	4.04	3.22	3.11	4.12	8.34
$\xi_0(s)$	1.99	2.68	2.33	2.09	3.88	4.32

Note: Parameter values as in figure 1, and $D_H = 0.1 = 10D_M$. Simulation results given in rows with “(s).” Measures of velocity during simulation depend on method used. We estimated velocity, obtaining $\xi_0(s)$, only after diffusion had taken a clearly circular shape.

Discussion

Our analysis introduces spatially detailed hypotheses to models for Lyme disease and other vector-borne infections with stage-structured dynamics and host dispersal. Regions where the incidence of human infection with *Borrelia* is high have expanded regularly, producing positive spatial correlation in disease measures at extended distances (Glanakov et al. 2001). Our results indicate that as we vary vector mortality rates, the velocity at which the disease advances is roughly proportional to the density of infectious vectors, hence proportional to the local risk of zoonotic infection. However, the spatial velocity of infection may increase or decrease with the density of infectious vectors as the rate at which juvenile ticks attack hosts varies. In either case, the velocity remains roughly proportional to the frequency of infection among hosts.

Most models for vector-borne disease ignore vector dynamics, and any stage structure, since infection among vectors may equilibrate faster than the host’s dynamics evolve (Dye and Williams 1995). However, the general implication of our results suggests that when the lifespan of host and vector scale similarly, R_0 for the pathogen depends on the way the vector’s stage-structured dynamics interact with host dispersal. Consequently, stage structure affects the criterion for pathogen invasion of a host population, the equilibrium frequency of infection among hosts, and the velocity of the spatial epidemic. A vector’s stage structure should remain significant when hosts are immobile and pathogen spread is due solely to dispersal by the vector, especially when acquisition and transmission of the pathogen occur in different stages. We simplified our analysis of the epidemic’s advance by assuming that total densities of host and vector were at equilibrium; vector dynamics are likely more important to the velocity of spatial advance when both vector abundance and the frequency of host infection are increasing.

To deduce hypotheses from the model, we focused on two effects, summarized in figures 1 and 2. First, recall that the equilibrium density of infectious vectors varies nonmonotonically with the mortality rate of adult ticks. Clearly, sufficient mortality among reproductives can reduce densities of all tick stages, and so inhibit the advance of infection. Density-dependent reproduction at low adult mortality remains a plausible but as yet uncertain assumption. Van Buskirk and Ostfeld (1995) impose a numerical upper bound for the number of ticks/host; some questing adults can then be excluded from reproduction. The sort of density-dependent crowding we assume might result from self-regulated recruitment caused by host immune responses to tick bites (Randolph 1979, 1994; Wikel 1982; Hughes and Randolph 2001). Host immune responses might decrease the average blood meal taken by adult female ticks, and individual tick fecundity varies directly with meal size (Hudson and Dobson 1995). But this effect is less certain than effects of abiotic factors on tick mortality (Mount et al. 1997).

Second, recall that at higher levels of the juvenile tick attack rate, the density of infectious vectors and the velocity of the epidemic’s advance vary inversely. So, the local risk of zoonotic infection declines while the spread of infection among vectors and hosts accelerates spatially. The effect simply means that an increased attack rate reduces the waiting time before a questing nymph encounters a mouse; the frequency of accidental bites to humans is consequently reduced. But our model’s assumption of continuous-time, mass-action development of ticks ignores seasonal pattern in abundances and activities of the different stages. Seasonal constraints on the appearance of emerging larvae might limit the spread of disease despite increased feeding success of infectious nymphs. Our model applies the same attack rate α to both larvae and the larger nymphs. Since ticks are relatively immobile, a juvenile tick’s opportunity to feed likely depends more on the density and mobility of mice than its own stage or size.

Finally, our model equates dispersal with random diffusion, an assumption difficult to fulfill at certain biological scales (Holmes 1993; Kot et al. 1996; Clark et al. 2001). But diffusion models often approximate dispersal data quite reasonably (van den Bosch et al. 1992) and so should predict the spatial advance of disease (Murray et al. 1986).

Acknowledgments

Discussion with F. Keesing, W. A. Maniatty, R. S. Ostfeld, and D. J. White was helpful. J.E.F. and T.K.O. thank the National Science Foundation for grant CCR-9896198. T.K.O. received further support from the National Science Foundation’s Vertical Integration of Research and Edu-

cation in the Mathematical Sciences (VIGRE) Program, through grant DMS-9983646.

Appendix

Stability of Demographic Equilibria

We assume the density of mice takes its locally stable, positive equilibrium $Q = K_M(1 - \mu_M/r_M)$. Demographic equilibrium refers to total densities of the various tick stages, without reference to infection. The variables are densities of adult ticks ($A^* + a^*$), questing larvae L^* , larvae infesting mice ($V^* + v^*$), and questing nymphs ($N^* + n^*$). At demographic equilibrium, the density of adult ticks is either 0 (tick extinction) or the positive density given by equation (10) in the text. The three other equilibrium values are directly proportional to $(A^* + a^*)$:

$$L^* = \frac{(\sigma + \mu_v)(\gamma + \alpha Q + \mu_N)\mu_A}{\sigma(\alpha Q)^2}(A^* + a^*), \quad (A1)$$

$$(V^* + v^*) = \frac{(\gamma + \alpha Q + \mu_N)\mu_A}{\sigma\alpha Q}(A^* + a^*), \quad (A2)$$

$$(N^* + n^*) = \left(\frac{\mu_A}{\alpha Q}\right)(A^* + a^*). \quad (A3)$$

Dynamics of the variables that sum susceptible and infective ticks are given by the sums of the dynamics for the two infection-status variables. The Jacobian for the tick demographic dynamics is the matrix **J** with elements j_{ik} :

$$\mathbf{J} = \begin{bmatrix} -\alpha Q - \mu_L & 0 & 0 & r[1 - 2c(A^* + a^*)] \\ \alpha Q & -\sigma - \mu_v & 0 & 0 \\ 0 & \sigma & -\gamma - \alpha Q - \mu_N & 0 \\ 0 & 0 & \alpha Q & -\mu_A \end{bmatrix}, \quad (A4)$$

where j_{14} is $\partial(dL/dt)/\partial(A + a)$ evaluated at equilibrium.

Existence of the positive equilibrium requires

$$\frac{r}{\mu_A} > \frac{(\alpha Q + \mu_L)(\sigma + \mu_v)(\gamma + \alpha Q + \mu_N)}{\sigma(\alpha Q)^2}. \quad (A5)$$

The tick birthrate r must be large enough, relative to adult mortality rate μ_A , to assure feasibility of the positive equilibrium. Otherwise, extinction is the only equilibrium.

We calculated the eigenvalues of **J** numerically for a range of μ_A and α values; other parameters were set as in the plots of figure 1. For any given μ_A , or any given α , extinction is the only feasible equilibrium, and is locally

stable, for r sufficiently small. Increased r makes the positive equilibrium feasible, and it is locally stable initially. Further increases in r destabilize the positive equilibrium.

Stability of Infection Equilibria

We assume the density of mice and the total densities of the various tick stages remain at positive equilibrium. The variables of interest are the equilibrium densities of infected mice, m^* , larvae feeding on infectious mice v^* , infectious nymphs n^* , and infected adults a^* . The infection equilibria are extinction of the spirochete, where each of the equilibrium densities is 0, and the positive equilibrium is given in the text. Maintenance of the cycle of infection requires $m^* > 0$. From equation (11), this becomes

$$\beta\beta_T\mu_A(A^* + a^*) > \mu_M Q. \quad (A6)$$

Maintaining *Borrelia* requires a greater r than necessary for feasibility of an equilibrium tick population in the absence of infection; compare expressions (A5) and (A6).

At aspatial equilibrium the Jacobian for the infection dynamics is the matrix

$$\mathbf{I} = \begin{bmatrix} -\beta\alpha n^* - \mu_M & 0 & \beta\alpha(Q - m^*) & 0 \\ \alpha L^* & -(\sigma + \mu_v) & 0 & 0 \\ 0 & \beta_T\sigma & -(\gamma + \alpha Q + \mu_N) & 0 \\ \alpha\beta_T N^* & 0 & \alpha Q - \alpha\beta_T m^* & -\mu_A \end{bmatrix}, \quad (A7)$$

where $L^* > 0$ questing larvae are susceptible. By column expansion $\det \mathbf{I} = -\mu_A \det G$, where G , with elements g_{ik} is the first three rows and columns of **I**.

At extinction of the spirochete, $g_{11} = -\mu_M$, and $g_{13} = \beta\alpha Q$. At the positive infection equilibrium these terms depend, respectively, on the density of infectious nymphs and the density of infected mice.

Local stability was determined from the characteristic equation of G , multiplied by -1 . The characteristic equation is $C(\lambda) = \lambda^3 + x_1\lambda^2 + x_2\lambda + x_3$, where λ is an eigenvalue and

$$\begin{aligned} x_1 &= -(g_{11} + g_{22} + g_{33}) > 0, \\ x_2 &= g_{11}g_{22} + g_{11}g_{33} + g_{22}g_{33} > 0, \\ x_3 &= -g_{11}g_{22}g_{33} - \alpha L^*\beta_T\sigma g_{13}, \end{aligned} \quad (A8)$$

where x_3 may be positive or negative. Local stability of either equilibrium, by the Routh-Hurwitz method, requires $x_1 > 0$, $x_1x_2 > x_3$, and $x_3 > 0$. The first condition is fulfilled at both spirochete extinction and the positive in-

fection equilibrium. The second, more complicated condition also holds at both equilibria. Local stability of each equilibrium, then, depends on the sign of x_3 .

Substituting equation (13) for L^* and simplifying shows that spirochete extinction is locally stable when

$$\mu_M Q > \beta \beta_T \mu_A (A^* + a^*). \quad (A9)$$

When this inequality is reversed, the positive equilibrium is locally stable; this condition recovers expression (A6). When the infection equilibrium is feasible, it is locally stable. Otherwise, spirochete extinction is stable.

Traveling Wave Velocity

The random variable X is distance a mouse disperses between its infection and passing the infection to a larval tick. The random variable T is the duration of the “typical” cycle of infection. Following Mollison (1991), the infection-dispersal kernel is

$$K(X, T) = \frac{\beta \alpha Q}{\gamma + \alpha Q + \mu_N} \beta_T \alpha L^* \frac{\sigma}{\sigma + \mu_V} \int_0^T \psi e^{-\psi(T-z)} e^{-\mu_M z} \phi_X(z) dz, \quad (A10)$$

where $\phi_X(z)$ is the normal probability density representing dispersal distance; $\phi_X(z)$ has mean 0 and variance proportional to time z . Simplifying the last expression yields

$$K(X, T) = R_0 \int_0^T \psi e^{-\psi(T-z)} \mu_M e^{-\mu_M z} \phi_X(z) dz. \quad (A11)$$

To calculate velocity we take the expectation of $\exp[\theta(X - \xi T)]$:

$$H(\xi, \theta) = R_0 \int_0^\infty \int_\Omega K(X, T) e^{\theta(X - \xi T)} dX dT. \quad (A12)$$

The smallest positive ξ for which $H(\xi, \theta) = 1$ is the minimal one-dimensional velocity (Mollison and Levin 1995). Mollison (1991) analyzes $H(\xi, \theta)$ when $K(X, T)$ has the form of (A10). Applying that method, let $p = (\mu_M E[T])^{-1}$; if ξ is a solution, ξ_0 is the associated standardized velocity. Define

$$h_1 = (1 - p)^{-1} - 2\xi_0^2,$$

$$h_2 = \frac{2\xi_0^2}{p(1 - p)}.$$

Then, we find ξ_0 numerically by solving

$$R_0 = 1 + \frac{2(h_1^2 + 3h_2)^{1.5} - 2h_1^3 - 9h_1 h_2}{27h_2}. \quad (A13)$$

For details, see Murray et al. (1986) and Mollison (1991).

Literature Cited

- Adjerid, S., B. Belguendouz, and J. E. Flaherty. 1999. A posteriori finite element error estimation for diffusion problems. SIAM (Society for Industrial and Applied Mathematics) Journal on Scientific Computing 21: 728–746.
- Andow, D. A., P. M. Kareiva, and S. A. Levin. 1990. Spread of invading organisms. Landscape Ecology 4:177–188.
- Aron, J. L., and R. M. May. 1982. The population dynamics of malaria. Pages 139–179 in R. M. Anderson, ed. Population dynamics of infectious diseases: theory and application. Chapman & Hall, London.
- Awerbuch, T. E., and S. Sandberg. 1995. Trends and oscillations in tick population dynamics. Journal of Theoretical Biology 175:511–516.
- Barbour, A. G., and D. Fish. 1993. The biological and social phenomenon of Lyme disease. Science (Washington, D.C.) 260:1610–1616.
- Bennett, C. E. 1995. Ticks and Lyme disease. Advances in Parasitology 36:343–405.
- Burgess, E. C., M. D. Wachal, and T. D. Clevon. 1993. *Borrelia burgdorferi* infection in dairy cows, rodents, and birds from four Wisconsin dairy farms. Veterinary Microbiology 35:61–77.
- Caraco, T., G. Gardner, W. Maniatty, E. Deelman, and B. K. Szymanski. 1998. Lyme disease: self-regulation and pathogen invasion. Journal of Theoretical Biology 193: 561–575.
- Clark, J. S., M. Lewis, and L. Horvath. 2001. Invasion by extremes: population spread with variation in dispersal and reproduction. American Naturalist 157:537–554.
- Diekmann, O., M. Gyllenberg, J. A. J. Metz, and H. R. Thieme. 1998. On the formulation and analysis of general deterministic structured population models. I. Linear theory. Journal of Mathematical Biology 36:349–388.
- Dunbar, S. R. 1983. Travelling wave solutions of diffusive Lotka-Volterra equations. Journal of Mathematical Biology 17:11–32.
- Dwyer, G. 1994. Density dependence and spatial structure of insect pathogens. American Naturalist 143:533–562.
- Dwyer, G., and J. S. Elkinton. 1995. Host dispersal and the spatial spread of insect pathogens. Ecology 76: 1262–1275.
- Dye, C., and B. G. Williams. 1995. Nonlinearities in the dynamics of indirectly-transmitted infections (or, does

- having a vector make a difference?). Pages 260–279 in B. T. Grenfell and A. P. Dobson, eds. *Ecology of infectious diseases in natural populations*. Cambridge University Press, Cambridge.
- Feng, Z., and J. X. Velasco-Hernández. 1997. Competitive exclusion in a vector-host model for dengue fever. *Journal of Mathematical Biology* 35:523–544.
- Gage, K. L., R. S. Ostfeld, and J. G. Olsen. 1995. Nonviral vector-borne zoonoses associated with mammals in the United States. *Journal of Mammalogy* 76:695–715.
- Glavanakov, S., D. J. White, T. Caraco, A. Lapenis, G. R. Robinson, B. K. Szymanski, and W. A. Maniatty. 2001. Lyme disease in New York state: spatial pattern at a regional scale. *American Journal of Tropical Medicine and Hygiene* 65:538–545.
- Holmes, E. E. 1993. Are diffusion models too simple? a comparison with telegraph models of invasion. *American Naturalist* 142:779–795.
- Holmes, E. E., M. A. Lewis, J. E. Banks, and R. R. Veit. 1994. Partial differential equations in ecology: spatial interactions and population dynamics. *Ecology* 75:17–29.
- Hudson, P. J., and A. P. Dobson. 1995. Macroparasites: observed patterns. Pages 14–176 in B. T. Grenfell and A. P. Dobson, eds. *Ecology of infectious diseases in natural populations*. Cambridge University Press, Cambridge.
- Hughes, V. L., and S. E. Randolph. 2001. Testosterone depresses innate and acquired resistance to ticks in natural rodent hosts: a force for aggregated distributions of parasites. *Journal of Parasitology* 87:49–54.
- Hutson, V. 1986. Stability in a reaction-diffusion model of mutualism. *SIAM (Society for Industrial and Applied Mathematics) Journal on Mathematical Analysis* 17:58–66.
- Jones, C. G., R. S. Ostfeld, E. M. Schaubert, M. Richard, and J. O. Wolff. 1998. Chain reactions linking acorns to gypsy moth outbreaks and Lyme-disease risk. *Science (Washington, D.C.)* 279:1023–1026.
- Kot, M., M. A. Lewis, and P. van den Driessche. 1996. Dispersal data and the spread of invading organisms. *Ecology* 77:2027–2042.
- Lewis, M. A., and P. Kareiva. 1993. Allee dynamics and the spread of invading organisms. *Theoretical Population Biology* 43:141–158.
- Mather, T. N. 1993. The dynamics of spirochete transmission between ticks and vertebrates. Pages 43–60 in H. S. Ginsberg, ed. *Ecology and environmental management of Lyme disease*. Rutgers University Press, Piscataway, N.J.
- Mollison, D. 1991. Dependence of epidemic and population velocities on basic parameters. *Mathematical Biosciences* 107:255–287.
- Mollison, D., and S. A. Levin. 1995. Spatial dynamics of parasitism. Pages 384–398 in B. T. Grenfell and A. P. Dobson, eds. *Ecology of infectious diseases in natural populations*. Cambridge University Press, Cambridge.
- Mount, G. A., D. G. Haile, and E. Daniels. 1997. Simulation of blacklegged tick (Acari: Ixodidae) population dynamics and transmission of *Borrelia burgdorferi*. *Journal of Medical Entomology* 32:461–484.
- Murray, J. D., E. A. Stanley, and D. L. Brown. 1986. On the spatial spread of rabies among foxes. *Proceedings of the Royal Society of London B, Biological Sciences* 229:11–151.
- Neubert, M. G., and H. Caswell. 2000. Demography and dispersal: calculation and sensitivity analysis of invasion speed for structured populations. *Ecology* 81:1613–1628.
- Ohsumi, T. K., J. E. Flaherty, V. H. Barocas, S. Adjerid, and M. Aiffa. 2000. Adaptive finite element analysis of the anisotropic biphasic theory of tissue-equivalent mechanics. *Computer Methods in Biomechanics and Biomedical Engineering* 3:215–229.
- Ostfeld, R. S., O. M. Cepeda, K. R. Hazler, and M. C. Miller. 1995. Ecology of Lyme disease: habitat associations of ticks (*Ixodes scapularis*) in a rural landscape. *Ecological Applications* 5:353–361.
- Ostfeld, R. S., F. Keesing, C. G. Jones, C. D. Canham, and G. M. Lovett. 1998. Integrative ecology and the dynamics of species in oak forests. *Integrative Biology: Issues, News & Reviews* 1:178–186.
- Piesman, J. 1988. Transmission of Lyme disease spirochetes. *Experimental and Applied Acarology* 7:71–80.
- Pound, J. M., J. A. Miller, J. E. George, and C. E. Lemelleur. 2000. The “4-poster” passive topical treatment device to apply acaricide for controlling ticks (Acari: Ixodidae) feeding on white-tailed deer. *Journal of Medical Entomology* 37:588–594.
- Randolph, S. E. 1979. Population regulation in ticks: the role of acquired resistance in natural and unnatural hosts. *Parasitology* 79:141–156.
- . 1994. Density-dependent acquired resistance to ticks in natural hosts, independent of concurrent infection with *Babesia microti*. *Parasitology* 108:413–419.
- Spielman, A., M. L. Wilson, J. F. Levine, and J. Piesman. 1985. Ecology of *Ixodes*-borne human babesiosis and Lyme disease. *Annual Review of Entomology* 30:439–460.
- Sutherst, R. W., K. B. W. Utech, M. J. Dallwitz, and J. D. Kerr. 1973. Intraspecific competition of *Boophilus microplus* (Canestrini) on cattle. *Journal of Applied Ecology* 10:855–862.
- Van Buskirk, J., and R. S. Ostfeld. 1995. Controlling Lyme disease by modifying the density and species composition of tick hosts. *Ecological Applications* 5:133–140.

- . 1998. Habitat heterogeneity, dispersal, and local risk of exposure to Lyme disease. *Ecological Applications* 8:365–378.
- van den Bosch, F., J. A. J. Metz, and O. Diekmann. 1990. The velocity of spatial population expansion. *Journal of Mathematical Biology* 28:529–565.
- van den Bosch, F., R. Hengeveld, and J. A. J. Metz. 1992. Analysing the velocity of animal range expansion. *Journal of Biogeography* 19:135–150.
- White, D. J. 1998. Lyme disease. Pages 141–153 in S. R. Palmer, Lord Soulsby, and D. I. H. Simpson, eds. *Zoonoses*. Oxford University Press, New York.
- White, D. J., H.-G. Chang, J. L. Benach, E. M. Bosler, S. C. Meldrum, R. G. Means, J. G. Debbie, G. S. Birkhead, and D. L. Morse. 1991. The geographic spread and temporal increase of the Lyme disease epidemic. *Journal of the American Medical Association* 266:1230–1236.
- Wikel, S. K. 1982. Immune responses to arthropods and their hosts. *Annual Review of Entomology* 27:21–48.
- Wilson, M. L., A. M. Ducey, T. S. Litwin, and A. Spielman. 1990. Microgeographic distribution of immature *Ixodes dammini* correlated with that of deer. *Medical and Veterinary Entomology* 4:151–159.

Editor: Joseph Travis
Associate Editor: Jim Bull